INFLUENCE OF ACOUSTIC EXCITATION ON AIRFOIL PERFORMANCE AT LOW REYNOLDS NUMBERS

S. Yarusevych*, J.G. Kawall and P. Sullivan***

***Department of Mechanical and Industrial Engineering, University of Toronto.**
****Department of Mechanical, Aerospace and Industrial Eng., Ryerson University.**

Keywords: *airfoil, separation, vortex shedding, low Reynolds number, wake, external acoustic excitation*

Abstract

The wake structure, vortex shedding characteristics and boundary-layer separation of a NACA 0025 airfoil and the effect of external acoustic excitations on airfoil performance were studied experimentally. Wind tunnel experiments were carried out for three Reynolds numbers and three angles of attack. Velocities were measured with hot-wires. Spectral analysis of these data was used in conjunction with complementary surface flow visualization to diagnose the performance of the airfoil at low Reynolds numbers. Evidence of wake vortex shedding and flow separation was obtained for most cases examined, and dependence of these phenomena on Reynolds number and angle of attack was found. The results establish that external acoustic excitation at a particular frequency and appropriate amplitude eliminates or reduces the separation region and decreases the airfoil wake, i.e., produces an increase of the lift and/or decrease of the drag. The acoustic excitation also alters the vortex shedding characteristics, decreasing the vortex length scale and the coherency of the vortex structure.

1 Introduction

The performance of airfoils at low Reynolds number flows has been of interest in connection with a wide range of applications including the operation of aircraft at low speeds and the design of micro air vehicles, compressor blades and inboard sections of helicopter rotors. Several investigators have studied airfoil performance in the low Reynolds number regime [1-3]. Their findings indicate that serious aerodynamic problems occur below a Reynolds number of approximately 200,000. Specifically, the laminar boundary layer on the upper surface of the airfoil is subjected to an adverse pressure gradient even at low angles of attack. This often results in either laminar boundary-layer separation and the formation of a large wake or boundary layer transition, reattachment and the formation of an extensive laminar separation bubble on the airfoil surface.

Laminar separation has a significant detrimental effect on airfoil lift and drag. Therefore, improving airfoil performance is of interest. This can be accomplished by introducing a flow control mechanism that serves to energize the boundary layer sufficiently to overcome the adverse pressure gradient and consequently reduce or suppress the separation bubble or the airfoil wake.

Relatively new methods of flow control involve the use of some kind of external periodic forcing. One such method is the excitation of the boundary layer with an acoustic source. Various studies have been performed showing that introduction of either external or internal acoustic excitation at an appropriate frequency to the airfoil boundary layer reduces the separation region and improves airfoil characteristics [3-9]. However, the complex physical mechanism responsible for this is not yet known in detail. Moreover, experiments in the low Reynolds number region are complicated by the measurable effect of the test section environment [2]. A disagreement of

experimental and numerical results [2] confirms the complexity of the combined phenomena. The increased sensitivity of low Reynolds number flows to the free stream conditions, angles of attack, airfoil shape and surface quality is well known and only adds uncertainty to the analysis of the control mechanism. Consequently, experimental attempts to predict optimum parameters of the excitation and explain the mechanism responsible for the control result in a wide range of sometimes contradictory conclusions.

The results and estimations of Zaman et al. [5], Hsiao et al. [9] and Nishioka et al. [8] indicate that the optimum effect occurs when the excitation frequency matches the instability frequency of the separated shear layer. However, at high angles of attack in the post-stall region, Hsiao et al. [9] have found that the most effective forcing frequency matches the vortex shedding frequency in the wake. At angles of attack around the onset of static stall, Zaman et al. [5] have reported that the excitation at certain frequencies actually decreased the lift coefficient. Significant differences in the optimum Strouhal number obtained in the various experiments have been reported by Zaman [7]. Furthermore, it has been concluded [4-7] that the effect and the effective frequency range of the excitation strongly depend on the excitation amplitude.

In most of the previous experimental studies, attention was concentrated on the boundary layer behavior or lift and drag measurements and the excitation effect. Wake structure and vortex shedding are also important aspects of airfoil performance. Huang and Lin [10] and Huang and Lee [11] did extensive experimental studies on vortex shedding and shear-layer instability in the low-Reynolds-number flow over a symmetrical airfoil. Vortex shedding development and characteristics were found to be closely related to boundary layer behavior, shear-layer instability, free stream conditions and angle of attack. In the references related to acoustic control, wake measurements, if any, were done at a single downstream location, with only the streamwise velocity component, and were briefly related to the improvement of airfoil performance.

The focus of the present work is to examine the effect of external acoustic disturbances on the boundary-layer separation, wake structure and vortex shedding of a NACA 0025 symmetrical airfoil for various Reynolds numbers and angles of attack.

2 Experimental Setup

Experiments were performed in the University of Toronto low-turbulence recirculating wind tunnel. The 5-m-long octagonal test section of this tunnel has a spanwise extent of 0.91 m and a height of 1.22 m. The flow enters the test section through seven screens and a 9:1 contraction. The operating velocity, U, is adjustable from 2.8 m/s to 18 m/s, with a free-stream turbulence intensity level less than 0.05%. One wall of the test section is made of Plexiglas for operational and visualization purposes. During the experiments, the free stream velocity was monitored by a pitot-static tube and set to the desired value by means of a calibrated hot-wire probe.

The performance of a symmetrical NACA 0025 aluminum airfoil with a chord length, c, of 0.3 m and a span of 0.88 m was examined for a range of chord Reynolds numbers (Re_c) and three angles of attack (α) of 10^o, 5^o, and 0^o. A schematic diagram of the test sections is shown in Fig.1. The airfoil was mounted horizontally in the test section 0.4 m downstream of the contraction. Sound excitation was provided by

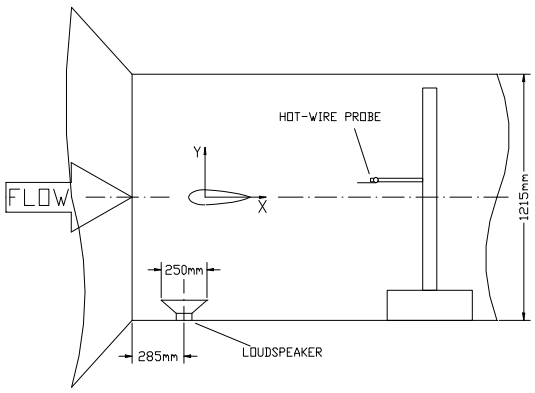

Figure 1. Tunnel test section.

means of a 250W loudspeaker mounted on the test section floor, under the leading edge of the airfoil. The mounting of the speaker was adjustable so as to either introduce vibrations to the structure along with sound waves or prevent vibrations of the structure, ensuring excitation solely from the sound. The speaker was driven through an amplifier by a variable-frequency wave generator. A Cartesian coordinate system was used, with x and y defined as shown in Fig.1 and the origin at the center of rotation of the airfoil.

Airfoil wake velocity data were obtained with constant temperature anemometers (Dantec 56C01 main units equipped with 56C17 CTA bridges). A Dantec 55P11 normal hot-wire probe and a Dantec 55P61 cross-wire probe were used separately to traverse vertical planes downstream of the airfoil. The probes were mounted on a remote-control traversing gear with a spatial resolution of 0.8 mm. For accurate detection of vortex-shedding frequencies, the probe position was adjusted in accordance with the Reynolds number and angle of attack. The output signals from the anemometers were acquired by a PC-based data acquisition system and stored for future calculations and analysis. Spectral analysis of the free-stream velocity signals established that there was no periodicity associated with the approach flow. To visualize boundary layer behavior, two rows of nylon tufts were installed on the airfoil surface 0.2 m away from the midspan in order to minimize their affect on the hot-wire measurements. Tests performed before and after installment of the tufts revealed no differences in the measurements.

3 Experimental Results

3.1 Flow Without Acoustic Excitation

The results presented herein pertain to the Reynolds numbers (Re_c) of $150x10^3$, $100x10^3$, and $57x10^3$ and the three angles of attack (α) of 10^o, 5^o, and 0^o. All three values of Re_c are within the low Reynolds number range; however, each of them produces different airfoil performance.

The boundary-layer-separation results were obtained via surface flow visualization to provide a qualitative picture of the boundary layer.

Boundary layer separation over a substantial portion of the upper surface of the airfoil took place at all three angles of attack for $Re_c=57x10^3$ and $Re_c=100x10^3$. The separation occurred over approximately 40% of the chord at $\alpha=0^o$, increasing to 50% at $\alpha = 5^o$, and reaching 60% at $\alpha=10^o$ for these two Reynolds numbers. A comparison of the extent of the separation regions for the two Reynolds numbers is not appropriate due to the poor sensitivity of the nylon tufts for $Re_c=57x10^3$ (compared to the sensitivity at the higher Reynolds numbers investigated). However, for $Re_c=150x10^3$, no evidence of boundary layer separation was found at $\alpha=0^o$ and $\alpha=5^o$, and only a small separation region was detected at the trailing edge, over 10-15% of the chord, at $\alpha=10^o$.

The airfoil boundary layer remained fully attached to the lower surface for all conditions considered except at $\alpha=5°$ for $Re_c=57x10^3$. In this case, the boundary layer separated at the trailing edge over 10% of the chord length.

Figure 2 shows typical mean wake velocity profiles ($\bar{u}/U$) for all three Reynolds numbers and angles of attack examined. It is evident that the mean profiles for $Re_c=57x10^3$ and $Re_c=100x10^3$ (Figs.2a and 2b) differ significantly from those for $Re_c=150x10^3$ (Fig. 2c). For the two lower Reynolds numbers, a wide wake is formed behind the airfoil with a maximum velocity deficit of approximately 0.65U at α =10° angle of attack. Note that the vertical location of the minimum velocity does not depend significantly on the angle of attack for the cases examined (Figs. 2a and 2b). The flow visualization results suggest that this is probably due to boundary layer separation on the upper side of the airfoil, which governs wake formation and structure. Unlike the situation for the two lower Reynolds numbers, for $Re_c=150x10^3$ (Fig. 2c), there is a narrower

mean profile with a maximum velocity deficit of 0.36U at 10° angle of attack. Moreover, as the angle of attack increases, the wake moves down, following the trailing edge. This behavior is similar to that of airfoil wakes at high Reynolds numbers without extensive boundary layer separation.

The width of the airfoil wake increases with increasing angle of attack. This appears to correlate with an increase of the separation region, as suggested by the visualization results. However, wake profiles for $Re_c=57x10^3$ at 0° and 5° angles of attack almost overlap at x/c=1 (Fig. 2a). This is thought to be the result of a partial boundary layer reattachment caused by an increase of the angle of attack, as observed by Mueller & Batill [3] and Zaman et al. [5] for two different airfoils with $Re_c=40x10^3$. However, such a reattachment was not detected via the present surface flow visualization due to the poor sensitivity of the tufts at low free-stream velocities. For the analysis of the organized flow structures, spectra of the wake velocity data are considered. Each of these spectra is normalized by the variance of the corresponding velocity component, so that the area under each spectrum is unity.

Figure 3 depicts spectra of the streamwise velocity component (E_{uu}) at x/c=2 for all Reynolds numbers and angles of attack examined. For the case of $Re_c=57x10^3$, a spectral peak centered at 8 Hz at all three angles of attack is clear evidence of vortex shedding in the airfoil wake (Fig. 3a). For this Reynolds number, the frequency of the vortex shedding does not appear to change, but the spectral peaks become sharper implying higher coherence in wake vortex structure, as angle of attack increases.

The spectral results for $Re_c=100x10^3$ (Fig. 3b) reveal a degree of dependency of vortex shedding on angle of attack. At $\alpha=0^o$, a wide peak centered at 20 Hz is evident. As the angle of attack increases to 5^o, a sharp peak centered at 20 Hz occurs (Fig. 3b). At $\alpha=10^o$, the vortex shedding frequency decreases (Fig. 3c), with the dominant spectral peak centered at 14 Hz. This indicates an increase in the length scale of the vortices, estimated as the ratio of free-stream velocity and the vortex-shedding frequency (U/f). No evidence of vortex shedding can be found for $Re_c=150x10^3$ at any angles of attack by means of a normal hot-wire probe (Fig. 3c). Nevertheless, a distinct Reynolds number dependency of the vortex shedding characteristics can be detected from a comparison of Figs. 3a and 3b. To be specific, the vortex shedding frequency steadily increases with increase of the Reynolds number. For example, at $\alpha=5^o$, the vortex-shedding frequency is f=8 Hz for $Re_c=57x10^3$ (Fig. 3b) and increases to f=20 Hz for $Re_c=100x10^3$ (Fig. 3b). Huang and Lin [10] and Huang and Lee [11] found a similar tendency in experiments with a NACA 0012 airfoil. Evidently, the characteristic length scale of the vortices

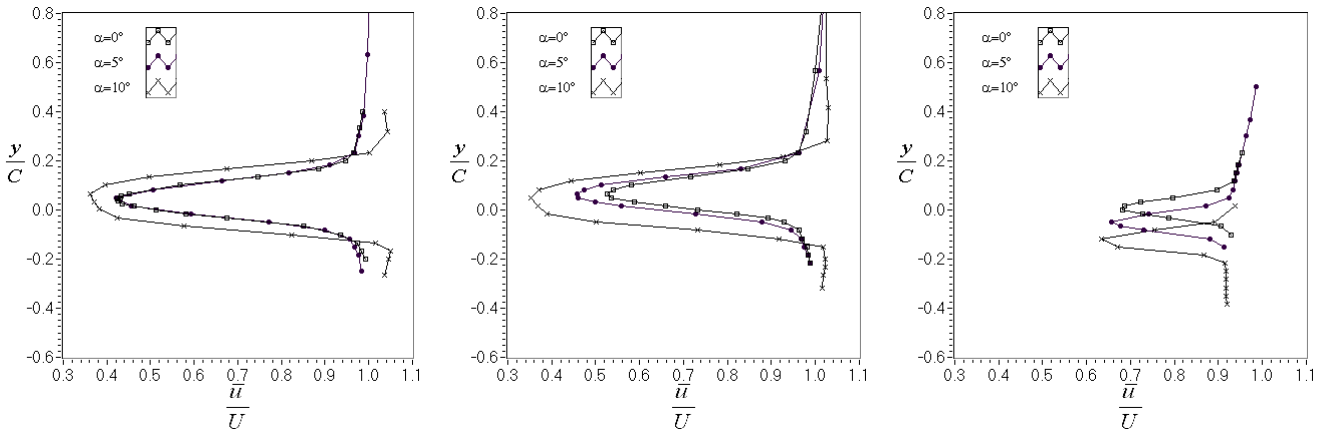

a) $Re_c=57x10^3$ b) $Re_c=100x10^3$ c) $Re_c=150x10^3$

Figure 2. Mean velocity profiles at x/c=1.

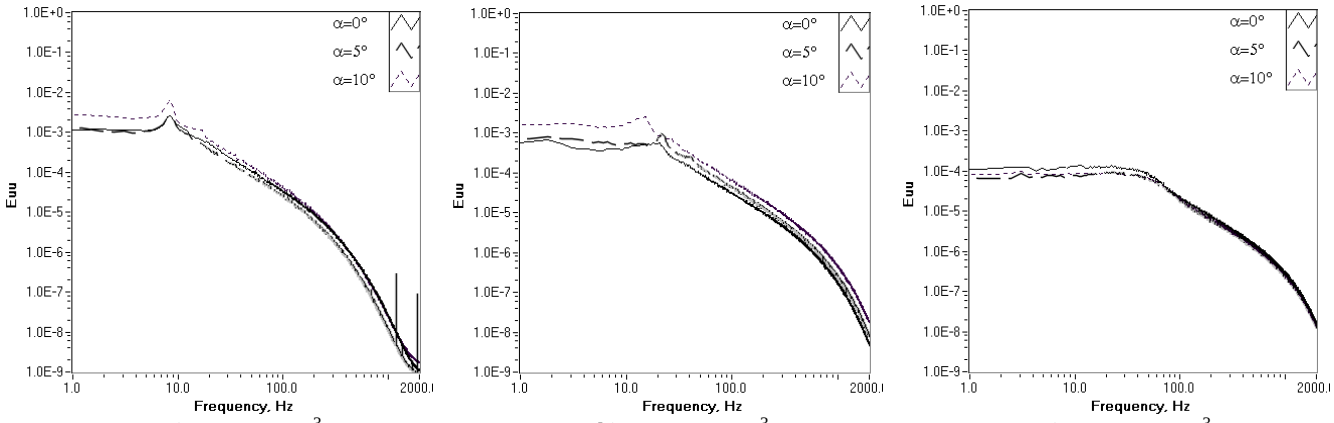

a) $Re_c=57x10^3$ b) $Re_c=100x10^3$ c) $Re_c=150x10^3$

Figure 3. E_{uu} spectra at x/c=2.

decreases with increase of the Reynolds number. Also, peaks in the spectra become wider and less defined, indicating lower coherency in the wake vortex structure as the Reynolds number increases.

2.4 Acoustic Excitation Effect

Two types of excitation were considered, viz., (i) acoustic excitation only, with the speaker isolated from the tunnel working section, and (ii) acoustic excitation with mechanical vibrations superimposed on the airfoil via the speaker.

The effect of external acoustic excitation on the separated boundary layer was first examined by means of flow visualization. The flow was excited at different frequencies with constant-amplitude acoustic excitation in presence of mechanical vibrations. For each of the cases examined, a range of frequencies (an effective-frequency range) was found to effect suppression of the separation region. This suppression occurred at some optimum excitation frequency with minimum power input. It should be noted that this type of excitation was found to be more effective in suppressing the separation region than "pure" acoustic excitation for $Re_c=57x10^3$.

The results summarized in Table 1 indicate the same trends as those obtained by others, i.e., an increase of the effective-frequency range with an increase of Reynolds number [6] and a decrease of the angle of attack [9]. Results from [9] also suggest that, for two different airfoils at low angles of attack ($\alpha \leq 6.5°$), the parameter $St_c/Re_c^{1/2}$, where St_c is the chord-based Strouhal number, ranges from 0.02 to 0.03 for the optimum excitation frequency. The values of this parameter obtained in the present work are 0.029 and 0.033 for $Re_c=57x10^3$ and 0.022 and 0.030 for $Re_c=100x10^3$ at $\alpha=0°$ and $\alpha=5°$, respectively (Table 1). All these values are within the indicated range, except the value at $\alpha=5°$ for $Re_c=57x10^3$ (which is 10% higher than the upper value).

The optimum excitation frequency increases as Reynolds number or angle of attack

α	0°			5°			10°		
Re_c	effect. freq. range (Hz)	optimum freq. (Hz)	$\frac{St_c}{Re_c^{1/2}}$	effect. freq. range (Hz)	optimum freq. (Hz)	$\frac{St_c}{Re_c^{1/2}}$	effect. freq. range (Hz)	optimum freq. (Hz)	$\frac{St_c}{Re_c^{1/2}}$
$57x10^3$	40-88	65	0.029	70-80	70	0.033	75-85	80	0.036
$100x10^3$	45-205	117	0.022	75-220	162	0.030	115-230	169	0.031
$150x10^3$	---------	---------	------	--------	---------	------	370-600	450	0.045

Table 1. Effective-frequency ranges and optimum frequencies.

increases. This frequency does not match the vortex shedding frequency, being an order of magnitude higher. It is speculated that the optimum frequencies found in the present investigation match the separated shear layer instability frequencies, which, as reported in the literature (e.g., [9]), are indeed approximately an order of magnitude higher than corresponding vortex-shedding frequencies. Note that only results pertaining to acoustic excitation applied at optimum frequencies are considered herein.

Figure 4 shows $\overline{u}/U$ profiles with and without acoustic excitations for Re_c=57x10^3 at x/c=2. As expected from the visualization results, acoustic excitation with superimposed structure vibrations significantly narrows the wake. Moreover, at α = 5° and 10°, the wake is shifted down following the incline of the trailing edge. For example, at α=10° (Fig. 4c), the location of the maximum wake deficit, which is decreased by the excitation from 0.23U to 0.2U, is shifted from y/c=0.1 to y/c=-0.2. "Pure" acoustic excitation is much less effective in narrowing the wake for this Reynolds number. Comparison of the profiles in Fig. 4 suggests that the "pure" acoustic excitation affects mainly the lower part of the wake. For this part of the wake, there is a decrease of the wake width at α=0° and α=5° (Figs. 4a and 4b). The wake is more affected at α=0°, i.e., it is diminished in size on both the upper and lower parts (Fig. 4a). At α=5° (Fig. 4b), this effect is only seen on the lower half of the flow with the upper half unaffected. At α=10° (Fig. 4c), the "pure" acoustic excitation does not seem to produce any effect at all. As a result of more

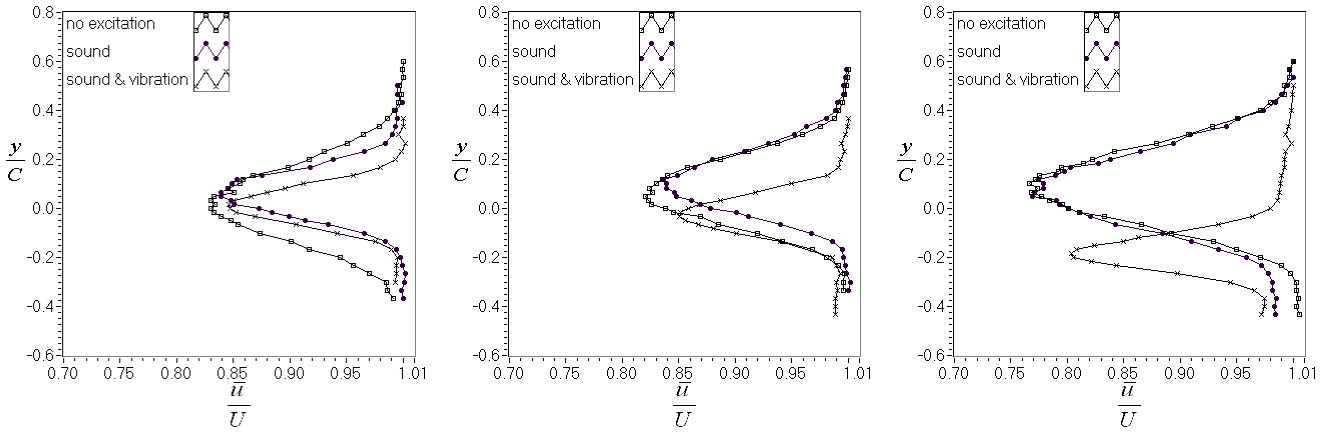

a) α=0° b) α=5° c) α=10°

Figure 4. Mean profiles with and without excitation for Re_c=57x10^3 and x/c=2.

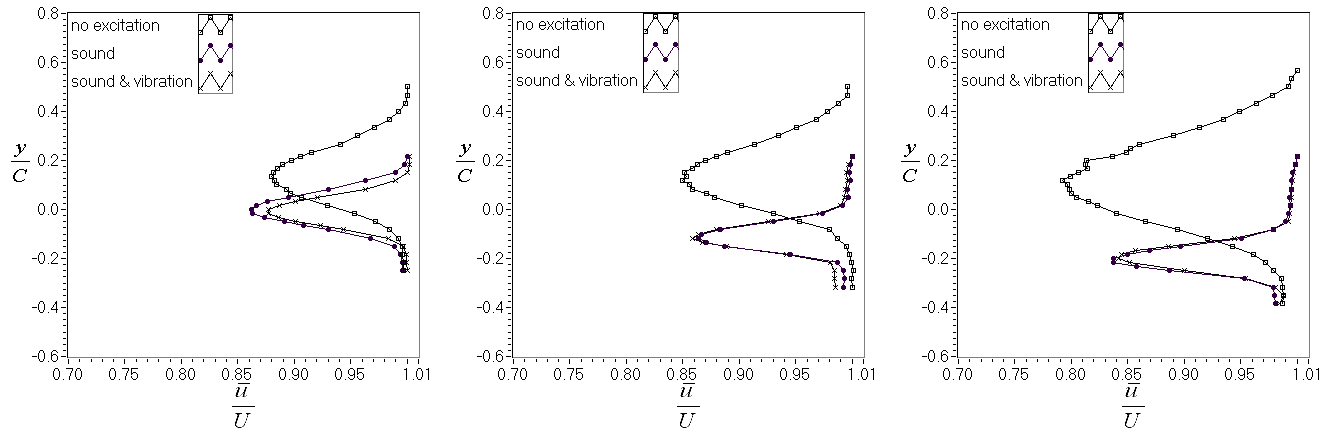

a) α=0° b) α=5° c) α=10°

Figure 5. Mean profiles with and without excitation for Re_c=100x10^3 and x/c=2

α	0°		5°		10°	
	Sound	Sound & Vibration	Sound	Sound & Vibration	Sound	Sound & Vibration
Re_c	$\frac{C_d}{C_{d0}}$	$\frac{C_d}{C_{d0}}$	$\frac{C_d}{C_{d0}}$	$\frac{C_d}{C_{d0}}$	$\frac{C_d}{C_{d0}}$	$\frac{C_d}{C_{d0}}$
$57x10^3$	0.6155	0.4756	0.8534	0.4873	0.9389	0.3574
$100x10^3$	0.7054	0.5580	0.3870	0.3946	0.2475	0.2525
$150x10^3$	---------	---------	---------	--------	0.7596	0.7610

Table 2. Normalized airfoil drag coefficients with and without excitation.

significant narrowing of the lower part of the wake at α=0° and α=5°, the position of the maximum velocity deficit shifts up slightly (Figs. 4a and 4b). This is due to the more significant effect of "pure" acoustic excitation on the boundary-layer separation on the lower surface of the airfoil than on the upper surface, as suggested by the visualization results.

Comparison of the mean profiles for $Re_c=100x10^3$ at x/c=2 in Fig. 5 reveals significant narrowing of the wake at all three angles of attack as a result of both types of excitation investigated. Moreover, the wake shifts down following the incline of the trailing edge at α=5° and α=10° (Figs. 5b and 5c), as in the case of the excitation with superimposed vibrations for $Re_c=57x10^3$. There is no apparent difference in the effect from the two types of the excitation on the profiles at α=5° and α=10° (Figs. 5b and 5c), as to be expected on the basis of the flow visualization results, and a small difference at α=0° (Fig. 5a). Similar results were obtained for $Re_c=150x10^3$ at α=10° and x/c=2. However, the extent of the effect is much smaller for this Reynolds number due to the suppression of a smaller separation region.

A quantitative analysis of the effect of acoustic excitation on airfoil performance is based on the drag coefficient results presented in Table 2. Note that airfoil drag coefficients (C_d) are normalized by the corresponding values of the drag coefficients calculated for the unexcited flow (C_{d0}), so that the normalized drag coefficients for the unexcited flow are unity. Clearly, the drag coefficients are lowered by either of the two types of excitation for all the cases examined. However, the acoustic excitation with mechanical vibrations is much more effective than the "pure" acoustic excitation in reducing the drag coefficient for $Re_c=57x10^3$. For example, at α=10°, the acoustic excitation of the flow with mechanical vibrations results in a decrease of the drag coefficient by about 64%, whereas the "pure" acoustic excitation results in a decrease of only 6.1% (Table 2). A more significant reduction of the drag coefficient is achieved for $Re_c=100x10^3$. The drag coefficient is reduced by about 75% by both types of excitation at α=10°.

It should be noted that for two lower Reynolds numbers, the more significant decrease of the drag coefficient becomes more pronounced as the angle of attack increases (Table 2). Ahuja & Burrin [4] reported a similar trend with respect to the effect of acoustic excitation on the lift coefficient. This trend is due to the suppression of the separation region, which increases as angle of attack increases.

For the highest Reynolds number tested, $Re_c=150x10^3$, the improvement of the airfoil performance is less significant than for the two lower Reynolds numbers. Nevertheless, a 24% decrease of the drag coefficient is achieved.

Spectra of the vertical velocity component (E_{vv}) are more sensitive to frequency-centered activity in wakes than are spectra of the streamwise velocity component (E_{uu}). For this reason only v-component spectra are considered in the discussion that follows. It should be noted

that spikes centered at the excitation frequencies and their harmonics appear in the E_{vv} spectra obtained with the disturbances present. Typical E_{vv} spectra for $Re_c=57x10^3$ at x/c=3 are shown in the Fig. 6. The sharp peak at 8 Hz in the unexcited flow at 0^o angle of attack (Fig. 6a) is attenuated by the "pure" acoustic excitation and shifted to 14 Hz. An increase of the angle of attack to 5^o (Fig. 6b) results in a smaller attenuation of the peak, with the vortex-shedding frequency shifted from 8 Hz to 10 Hz. A further increase of the angle of attack to 10^o, results in the spectrum being only slightly altered by the acoustic excitation, with the vortex-shedding frequency shifted to 8.5 Hz (Fig 6c). These observations suggest that the vortex shedding is influenced by acoustic excitation at optimum frequencies, which cause a decrease of the vortex length scale and coherence. The weakening of this effect and the narrowing of the effective frequency range as angle of attack increases is in a good agreement with the results of Hsiao et al. [9]. The effect of acoustic excitation in conjunction with mechanical vibrations differs significantly from the effect of "pure" acoustic excitation for this Reynolds number (Fig. 6). The corresponding spectra, which are shown as long dashed curves, display distinct peaks centered at 16.5 Hz, 15.5 Hz and 15 Hz, representing vortex shedding frequencies at 0^o, 5^o and 10^o angles of attack, respectively. The angle-of-attack effect is substantially diminished in this case, as the energy of the vortices and the shedding frequency do not change significantly with increase of α. Figure 7 shows E_{vv} spectra for

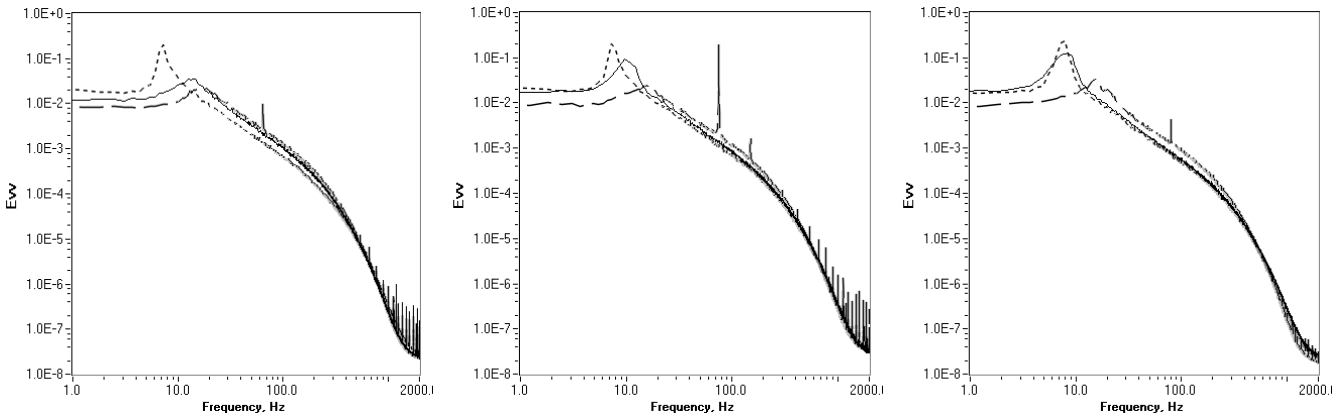

a) α=0° b) α=5° c) α=10°

Figure 6. E_{vv} spectra with and without excitation for $Re_c=57x10^3$; x/c=3.
_ _ _ _ _, no excitation , _____ , sound; _ _ _ , sound and vibrations.

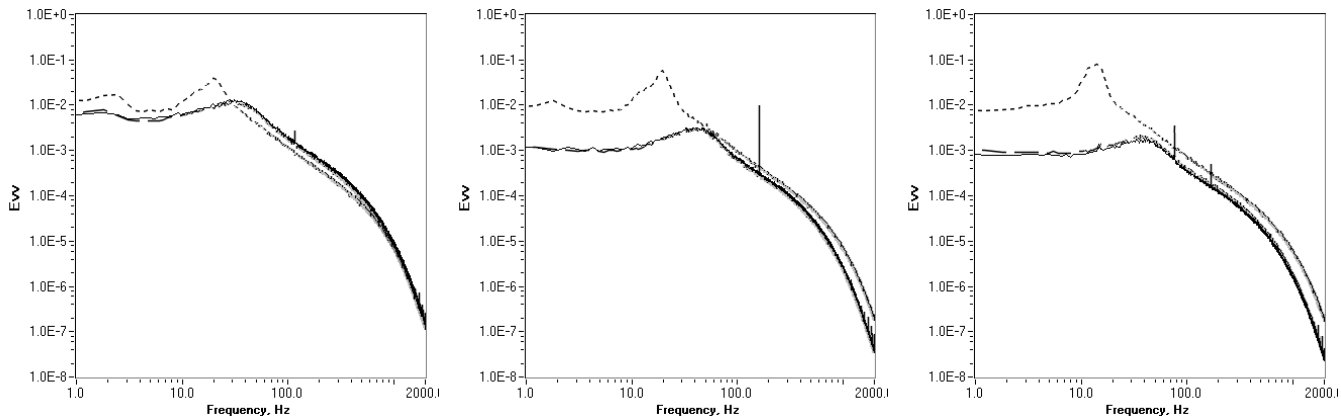

a) α=0° b) α=5° c) α=10°

Figure 7. E_{vv} spectra with and without excitation for $Re_c=100x10^3$; x/c=3. (see caption for Fig. 6)

Re_c=100x10^3 at x/c=3. The peaks in the spectra associated with the unexcited flow are attenuated, broadened and shifted to higher frequency values by either of the two types of the excitation studied. Note that the extent of these effects for this case is much greater than for the Re_c=57x10^3 case. The peaks corresponding to 0^o, 5^o and 10^o angles of attack that are centered at 20 Hz, 20 Hz and 14 Hz are strongly attenuated and shifted to 30 Hz, 40 Hz and 40 Hz, respectively. Thus, the length scale of the vortices and coherency of the shedding are substantially decreased.

As in the case of the mean velocity profiles, spectra pertaining to "pure" acoustic excitation and acoustic excitation with mechanical vibrations show significant overlap in Fig. 6 at corresponding angles of attack. This suggests that there is no difference in the effect of these two types of excitation on vortex shedding, which is to be expected from the flow visualization results, indicating that both types of acoustic excitation produce full reattachment. Moreover, the effect of the acoustic excitation on the vortex shedding for this Reynolds number corresponds to the effect on the drag coefficient, as more significant diminishment of the peaks in the spectra is achieved for higher angles of attack.

The results for Re_c=150x10^3 at x/c=3 and 10^o angle of attack are presented in the Fig. 8. A broad peak centered at 68 Hz is evident in the unexcited flow spectrum that could not be detected in the E_{uu} spectrum. Thus a weak vortex shedding occurs. As in the case of Re_c=100x10^3, the peak in the unexcited spectrum is attenuated by either type of the excitation and shifted to 80 Hz.

From a comparison of the spectral results and the previously discussed findings, it is concluded that the magnitude of the acoustic excitation effect on the vortex shedding of the airfoil correlates with the improvement in the airfoil performance, i.e., an increase of the lift and/or a decrease of the drag. Therefore, the effect of acoustic excitation on airfoil performance can be assessed by comparing spectral results obtained with and without this excitation.

4 Conclusions

Performance of a NACA 0025 airfoil at low Reynolds numbers was studied experimentally by means of hot-wire velocity measurements and complementary surface flow visualization.

Boundary layer separation takes place over a substantial region on the upper surface of the airfoil at all three angles of attack for Re_c=57x10^3 and Re_c=100x10^3 and only over a small region at α=10° for Re_c=150x10^3. This results in the formation of much wider wakes for the two lower Reynolds numbers compared to the case for Re_c=150x10^3 at the corresponding angles of attack.

Vortex shedding was detected for most Reynolds numbers and angles of attack examined. The results demonstrate that the shedding characteristics depend strongly on Reynolds number. Specifically, the shedding frequency increases and the vortex length scale and coherency decrease as Reynolds number increases. A weaker dependence of these characteristics on the angle of attack was found.

External acoustic excitation at particular frequencies and appropriate amplitudes with and without structure vibrations can substantially reduce or suppress the separation region so that an increase in lift and/or a decrease in drag result.

The effect of the excitation strongly depends on the excitation frequency and

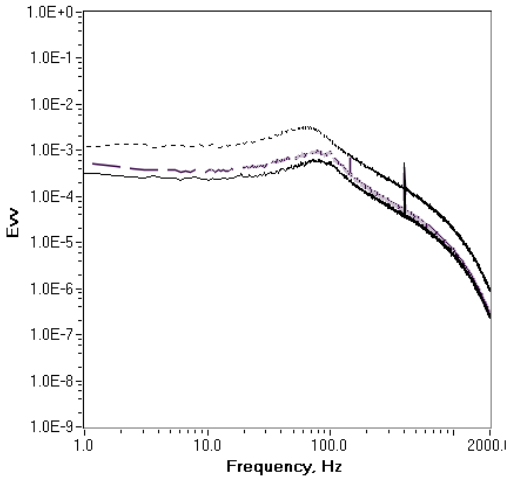

Figure 8. E_{vv} spectra with and without excitation for Re_c=150x10^3; x/c=3; α=10°. (see caption for Fig. 6)

amplitude. The effective frequency range decreases with a decrease of the excitation amplitude. For a constant amplitude excitation, this range narrows with a decrease of the Reynolds number or increase of the angle of attack. The best effect is achieved at an optimum frequency, which increases as Reynolds number or angle of attack increases. It is speculated that the optimum frequencies found in this investigation match separated shear-layer instability frequencies.

The acoustic excitation alters the vortex shedding characteristics, decreasing the vortex length scale and the coherency of the vortex structure. Moreover, the magnitude of the acoustic excitation effect on the vortex shedding correlates with the extent of the improvement in the airfoil performance, i.e., an increase in the lift and/or a decrease in the drag.

Evidently, for the same power input into the loudspeaker, more energy is transferred to excite the flow in the case of acoustic excitation in conjunction with superimposed vibrations than in the case of acoustic excitation alone. Nevertheless, the results suggest that there is little difference between the effects of two types of excitation on the airfoil performance for $Re_c=100x10^3$ and $Re_c=150x10^3$. In contrast, there is a substantial difference between the effects for $Re_c=57x10^3$, with the acoustic excitation in the presence of structure vibrations being more effective. Hence, higher energy is required to produce a significant effect on airfoil performance for $Re_c=57x10^3$ than for the two higher Reynolds numbers; however, an increase of the energy used to excite the flow for $Re_c=100x10^3$ and $Re_c=150x10^3$ does not result in an enhancement of airfoil performance. This suggests that once the separation region is suppressed by the acoustic excitation with a certain amplitude, further increase of the excitation amplitude does not significantly affect airfoil performance. Furthermore, it can be concluded that higher amplitude excitations are needed to influence the airfoil performance at lower Reynolds numbers.

5 Acknowledgement

The authors wish to thank Mr. Jerry Karpynczyk for his help with the experimental setup. This research was supported by the Natural Science and Engineering Research Council of Canada through operating and equipment grants.

References

[1] Lissaman P B S. *Low Reynolds number airfoils.* Annual Review of Fluid Mechanics, Vol. 15, pp. 223-239, 1983.

[2] McGhee R J, Walker B S and Millard B F. *Experimental results for the Eppler 387 airfoil at low Reynolds numbers in the Langley low-turbulence pressure tunnel*. NASA TM-4062, 228 p., 1988.

[3] Mueller T J and Batill S M. *Experimental studies of separation on a two-dimensional airfoil at low Reynolds numbers.* AIAA Journal, Vol. 20, No. 4, pp. 457-464, 1982.

[4] Ahuja K K and Burrin R H. *Control of flow separation by sound.* AIAA paper No. 84-2298, 1984.

[5] Zaman K B M Q, Bar-Sever A and Mangalam S M. *Effect of acoustic excitation on the flow over a low-Re airfoil.* Journal of Fluid Mechanics, Vol. 182, pp. 127-148, 1987.

[6] Zaman K B M Q and McKinzie D J. *Control of laminar separation over airfoils by acoustic excitation.* AIAA Journal, Vol. 29, No. 7, pp. 1075-1083, 1991.

[7] Zaman K B M Q. *Effect of acoustic excitation on stalled flows over an airfoil.* AIAA Journal, Vol. 30, No. 6, pp. 1492-1499, 1992.

[8] Nishioka M, Asai M and Yoshida S. *Control of flow separation by acoustic excitation.* AIAA Journal, Vol. 28, No. 11 pp. 1909-1915, 1990.

[9] Hsiao F B, Jih J J and Shyu R N. *The effect of acoustics on flow passing a high-AOA airfoil*. Journal of Sound and Vibration, Vol. 199, No. 2, pp .177-178, 1997.

[10] Huang R F and Lin C L. *Vortex shedding and shear-layer instability of wing at low-Reynolds numbers*. AIAA Journal, Vol. 33, No. 8, pp. 1398-1430, 1995.

[11] Huang R F and Lee H W. Turbulence effect on frequency characteristics of unsteady motions in wake of wing. AIAA Journal, Vol. 38, No. 1, pp. 87-94, 2000.